Electrochemical study of the Eu(III)/Eu(II) system in molten fluoride media

L. Massot*, P. Chamelot, L. Cassayre, P. Taxil

Université de Toulouse ; INPT, UPS ; Laboratoire de Génie Chimique ; Département Procédés Electrochimiques ; F-31062 Toulouse cedex 09, France

CNRS ; Laboratoire de Génie Chimique ; F-31062 Toulouse cedex 09, France

(*) corresponding author:

Massot Laurent
Tel: +33 5 61 55 81 94
Fax: +33 5 61 55 61 39
E-mail: massot@chimie.ups-tlse.fr

Abstract

The electrochemical behaviour of the Eu(III)/Eu(II) system was examined in the molten eutectic LiF-CaF_2 on a molybdenum electrode, using cyclic voltammetry, square-wave voltammetry and chronopotentiometry. It was observed that EuF_3 is partly reduced into EuF_2 at the operating temperatures (1073-1143 K). The electrochemical study allowed to calculate both the equilibrium constant and the formal standard potential of the Eu(III)/Eu(II) system. The reaction is limited by the diffusion of the species in the solution; their diffusion coefficients were calculated at different temperatures and the values obey Arrhenius' law. The second system Eu(II)/Eu takes place out of the electrochemical window on an inert molybdenum electrode, which inhibits the extraction of Eu species from the salt on such a substrate.

Key words

Molten fluorides, europium, cyclic voltammetry, square wave voltammetry, formal standard potential

1. Introduction

Partitioning and transmutation (P&T) concepts are acknowledged as efficient ways to reduce the long-term radiotoxicity of nuclear wastes by multi-recycling of actinides (An) [1]. These concepts require the separation of the An to be recycled from the fission products present in the spent nuclear fuel. For this purpose, hydrometallurgical processes are being developed in order to improve the currently used Purex process which allows to recover U and Pu, but not the higher An such as Am and Cm.

Pyrochemical processes involving molten salts solvents (mostly fluoride and chloride based media) are considered as a suitable alternative to aqueous processes in the view of the separation of An from the fission products. Electrochemical based methods (electrorefining, electrolysis) and reductive extraction are the main operations currently studied for the separation [2]. Though, success in the development of pyrochemical processes requires reliable data on the electrochemical behaviour and thermodynamic data of both An and fission products dissolved in molten salt solvents. Among the fission products, the lanthanides (Ln) such as Ce, Sm, Nd, Eu, Gd, Dy have very comparable chemical properties with the An, which makes the An-Ln separation very difficult. Furthermore, in order to ensure a longer lifetime of the solvents used in these processes, the decontamination of the fluoride salt from the Ln is also a key issue. On top of these P&T concepts, the Molten Salt Reactor (one of the six nuclear reactors concept evaluated in the frame of the Generation IV Forum), which should operate with fluoride molten salts, requires an online reprocessing in order to remove fission products and particularly Ln [3].

Due to these on-going research topics, a specific attention is required to determine the properties of Ln dissolved in molten fluoride salts. In our previous studies, the behaviour of Sm, Nd and Gd ions [4] was determined in molten fluoride salts. The study presented here is focused on the behaviour of the Eu element in the molten fluoride eutectic LiF-CaF_2. The possibility of extracting Eu species by electrodeposition from this specific solvent is evaluated, since the LiF-CaF_2 melt exhibits one of the largest electrochemical windows among fluoride mixtures below 1273 K [5].

To the authors' knowledge, there is no study concerning the behaviour of Eu ions in molten fluoride media available in the literature. However, Eu species have been studied in chloride media: S. Kuznetsov *et al.* used NaCl–KCl, KCl and CsCl media to investigate Eu electrochemical behaviour in the 973 – 1123 K temperature range [6-8]. These authors

observed that both $EuCl_3$ and $EuCl_2$ were present in the melt at equilibrium. $EuCl_2$ was assumed to be formed during the heat treatment, according to the following reaction, as observed above 570 K by D.M. Laptev *et al.* [9]:

$$EuCl_3 \leftrightarrows EuCl_2 + \tfrac{1}{2} Cl_2 \qquad (1)$$

It was also shown that only the first step of the electrochemical reduction process of $EuCl_3$, diffusion controlled, can be observed in molten chloride on a molybdenum electrode:

$$EuCl_3 + e^- \leftrightarrows EuCl_2 + Cl^- \qquad (2)$$

Indeed, the prior reduction of Li(I) ions from the solvent hinders the reduction of $EuCl_2$ into Eu metal and, herein, makes impossible the extraction of metallic Eu from the molten solution. This observation was confirmed by Bermejo *et al.* in the molten LiCl-KCl eutectic salt [10].

The present work deals with the electrochemical properties of the Eu ions in the LiF-CaF_2 mixture, in the 1073 – 1173 K temperature range, studied with transient electrochemical techniques (cyclic voltammetry, chronopotentiometry and square wave voltammetry) on an inert molybdenum electrode. The feasibility of Eu extraction by electrodeposition in fluoride melts is assessed, as well as thermodynamic data such as: (i) the formal standard potential of the Eu(III)/Eu(II) system and (ii) the diffusion coefficients of Eu(III) and Eu(II).

2. Experimental

- The cell consisted of a vitreous carbon crucible placed in a cylindrical vessel made of refractory steel and closed by a stainless steel lid cooled by circulating water [11-12]. The inner part of the cell walls was protected against fluoride vapours by a graphite liner. The experiments were performed under an inert argon (less than 5 ppm O_2) atmosphere, previously dehydrated and deoxygenated using a purification cartridge (Air Liquide). The cell

was heated using a programmable furnace and the temperatures were measured using a chromel-alumel thermocouple.

- The electrolytic bath consisted of a eutectic LiF-CaF_2 (Merck 99.99%) mixture (77/23 molar ratio). Before use, it was dehydrated by heating under vacuum (10^{-2} mmHg) from ambient temperature up to its melting point (1035 K) for 48 hours. Eu ions were introduced into the bath in the form of powder of europium trifluoride, EuF_3 (Merck 99.99%).

- Electrodes: a molybdenum wire (1 mm diameter) was used as working electrode. Molybdenum was chosen because of its inertness with respect to europium: according to the Mo/Eu binary diagram [13], there is no intermetallic compound in the working temperature range. The active surface of the Mo electrode was determined after each experiment by measuring the immersion depth in the bath. The auxiliary electrode was a vitreous carbon (V25) rod (3 mm diameter) with a large surface area (2.5 cm^2). The potentials were referred to a platinum wire (0.5 mm diameter) immersed in the molten electrolyte, acting as a quasi-reference electrode $Pt/PtO_x/O^{2-}$ [14].

- Electrochemical equipment: all electrochemical studies and electrolysis were performed with an Autolab PGSTAT30 potentiostat / galvanostat controlled by the research software GPES 4.9.

- Electrochemical techniques: cyclic voltammetry, chronopotentiometry and square wave voltammetry were the electrochemical techniques used for the investigation of the Eu redox system.

3. Results

3.1 Cyclic voltammetry

Cyclic voltammetry was carried out on a molybdenum electrode in a solution of EuF_3 in a LiF-CaF_2 melt at 1073 K. The electrochemical window offered by the LiF-CaF_2 solvent is

comprised between the reduction of lithium ions and the anodic dissolution of the molybdenum electrode.

The cyclic voltammogram obtained at 100 mV s^{-1} on a Mo electrode at T = 1073 K, shown in Figure 1, exhibits two peaks (I_a and I_c) at around 0 V and 0.25 V versus the platinum comparison electrode in the cathodic and anodic runs respectively, whatever the potential scanning sense. The shape of these peaks suggests that both the reduction and the oxidation products are soluble. The peaks I_c and I_a are attributed to the reduction of Eu(III) into Eu(II) and the oxidation of Eu(II) into Eu(III) respectively:

$$Eu(III) + e^- \leftrightarrows Eu(II) \qquad (3)$$

$$Eu(II) \leftrightarrows Eu(III) + e^- \qquad (4)$$

Moreover, the significant anodic current, observed for potentials higher than the potential peak (I_a), suggests the presence of Eu(II) ions in the mixture, while only Eu(III) was introduced initially. This reminds similar observations performed in chloride systems by Laptev *et al.* and Kuznetsov *et al.* [6-9]: as mentioned before, these authors explained the formation of Eu(II) in the molten salt by the dissociation of $EuCl_3$ into $EuCl_2$ and Cl_2 above 570 K.

A similar reaction could explain the partial spontaneous reduction of EuF_3 into EuF_2:

$$EuF_3 \leftrightarrows EuF_2 + \tfrac{1}{2} F_{2(g)} \qquad (5)$$

Even if the thermodynamic properties of pure Ln trifluorides are quite well established [15], the data concerning Ln dihalides are rather scarce and mostly based on thermodynamic predictions. However, Bratsch and Silber have shown that only SmF_2, YbF_2 and EuF_2 should be stable as Ln difluorides and that among them EuF_2 was the most stable [16]. This supports our experimental observation, which shows that dissolved Eu(II) is stable on a large potential range (about 2 V) in the molten LiF-CaF_2 mixture.

Finally, it can also be noted from the cyclic voltammogram that the reduction of Eu(II) into Eu is not observed prior to the solvent reduction.

3.2 Square wave voltammetry

In order to confirm this electrochemical behaviour, square wave voltammetry was used to determine the number of exchanged electrons for peak I_a and I_c, because of a better accuracy of this method [11].

The application of the square wave voltammetry technique has already been detailed in previous work [11]. The mathematical analysis of the obtained peaks yields, in the case of a reversible system, a simple equation associating the half-width of the peak $W_{1/2}$ and the number of exchanged electrons [17-18]:

$$W_{1/2} = 3.52 \frac{RT}{nF} \qquad (6)$$

Where n is the number of exchanged electrons, F is the Faraday's constant, R is the gas constant and T is the absolute temperature in K.

Figure 2 shows two square wave voltammograms of the LiF-CaF_2-EuF_3-EuF_2 system on a molybdenum electrode at 1073 K: the anodic one was plotted from -0.6 to 0.6 V vs. Pt, and the cathodic one was plotted from 0.6 to -0.6 V vs. Pt. Two symmetrical peaks can be observed at 0.05 V vs. Pt, corresponding to $E_{p/2}$ for the cyclic voltammogram, and indicating that the system Eu(III)/Eu(II) is reversible.

The validity of application of Eq. (6) was verified by plotting the current density of the peak versus the square root of the frequency as reported in previous works [19-20]. Here, a linear relationship was observed in the 9 – 100 Hz frequency range.

According to Eq. (6), the measurement of $W_{1/2}$ leads to a number of exchanged electrons equal to 1 for the reduction and oxidation peaks. This result confirms that the

reduction of Eu(III) in LiF-CaF_2 melts yields a divalent europium compound Eu(II) and the oxidation of Eu(II) yields to Eu(III).

3.3 Chronopotentiometry

In order to confirm the diffusion control of the Eu(III)/Eu(II) reduction process, several chronopotentiograms were measured on a molybdenum electrode at 1073 K. Typical chronopotentiograms plotted in Figure 3 for Eu(III) reduction (I_{app} = -15 mA) and Eu(II) oxidation (I_{app} = 10 mA) exhibit a single plateau at about – 0.15 V vs. Pt and 0.15 V vs. Pt, corresponding to the Eu(III)/Eu(II) electrochemical system. Several curves have been plotted for various applied intensities. According to Sand's law [21], the ratio $\frac{I\sqrt{\tau}}{C^\circ}$ versus I for each system has to be constant.

$$\frac{I\sqrt{\tau}}{C^\circ} = -\,0.5\ n\ F\ S\ (\pi\ D)^{1/2} = \text{constant} \qquad (7)$$

Where S is the electrode surface area and D the diffusion coefficient.

The data plotted in Figure 4 prove that this equation is verified both for Eu(III) reduction and Eu(II) oxidation. These experiments were repeated at various temperatures and confirmed the validity of equation (7). The Eu(III)/Eu(II) system is then diffusion controlled.

4. Discussion

4.1 Eu(III)/Eu(II) equilibrium constant

The concentration ratio $\frac{[Eu(II)]}{[Eu(III)]}$ in the LiF-CaF_2-EuF_3-EuF_2 mixture was calculated by comparing the surface area of the SWV peaks of the Eu(III) reduction and Eu(II) oxidation respectively. For this measurement, square wave voltammetry was preferred since, as

mentioned above, it is more accurate than cyclic voltammetry to determine surface area of voltammograms peaks. By integrating the SWV peak areas and using the Faraday law, it is possible to determine the concentrations of Eu(III) and Eu(II) in the melt: the anodic and cathodic peaks surface areas are proportional to the Eu(II) and Eu(III) contents respectively:

$$A_{I_a} = n_{e^-} * F * m * [Eu(II)] \quad (8)$$

$$A_{I_c} = n_{e^-} * F * m * [Eu(III)] \quad (9)$$

Where m is the mass of solvent and [ ] stands for the concentration in mol kg^{-1}.

Consequently, the following relationship can be written:

$$A_{I_a} / A_{I_c} = \frac{[Eu(II)]}{[Eu(III)]} = K° \quad (10)$$

At T = 1073 K, the measured data gives K° = 0.811 ± 0.002, which confirms the presence of Eu(II) ions in the solution under equilibrium conditions. The same methodology was applied to evaluate the dependency of the equilibrium constant K° with temperature. The results obtained for four temperatures are gathered in Table 1: the clear trend is that the concentration ratio increases with temperature, which indicates an enhancement of the decomposition reaction (Eq. 5) of EuF_3.

The determination of K° was used to plot a calibration curve including the linear relationship between δI_{pa} and [Eu(II)] on one hand and δI_{pc} and [Eu(III)] on the other hand using square waves voltammograms performed at 25 Hz. Figure 5 shows these two relationships on Mo electrode at 1073 K for various Eu(II) and Eu(III) contents.

4.2. Eu(III)/Eu(II) formal standard potential

The standard potential of the Eu(III)/Eu(II) system was calculated by applying the Nernst' law to Eq. (3):

$$E_{I=0} = E^{o}_{Eu(III)/Eu(II)} + \frac{RT}{F} \ln\left(\frac{a_{Eu(III)}}{a_{Eu(II)}}\right) \quad (11)$$

Where $a_i = \gamma_i * (C_i / C°)$ is the activity of the specie i, γ_i is the activity coefficient, C_i is in mol kg^{-1} and C° (the standard concentration) is equal to 1 mol kg^{-1}.

So, Eq. (11) can be written:

$$E_{I=0} = E^{o}_{Eu(III)/Eu(II)} + \frac{RT}{F}\ln\left(\frac{\gamma_{Eu(III)}}{\gamma_{Eu(II)}}\right) + \frac{RT}{F}\ln\left(\frac{[Eu(III)]}{[Eu(II)]}\right) \qquad (12)$$

The formal standard potential can then be expressed:

$$E^{*}_{Eu(III)/Eu(II)} = E^{o}_{Eu(III)/Eu(II)} + \frac{RT}{F}\ln\left(\frac{\gamma_{Eu(III)}}{\gamma_{Eu(II)}}\right) \qquad (13)$$

Consequently, the values of the equilibrium potential, measured by open-circuit chronopotentiometry, allowed calculating, for each operating temperature, the formal standard potential of Eu(III)/Eu(II) system. The unit conversion of equilibrium potentials from V vs. Pt to V vs. $F_{2(g)}/F^-$ was realized using the Li(I)/Li reduction potential ($E_{Li(I)/Li}$). This potential $E_{Li(I)/Li}$ was calculated in V vs. $F_{2(g)}/F^-$ using thermodynamic data (HSC Chemistry software) and measured in V vs. Pt on the cyclic voltammogram.

The average of our measurements is gathered in Table 2: the values are comprised between -3.53 V vs. F_2/F^- at 1073 K and -3.33 V vs. F_2/F^- at 1143 K.

4.3 Diffusion coefficient of Eu(III) and Eu(II) ions

4.3.1 Using cyclic voltammetry

$D_{Eu(III)}$ and $D_{Eu(II)}$ were first calculated by plotting cyclic voltammograms at several scan rates. The cathodic and the anodic peak intensities are correlated with the potential scan rate by the following relationship (Randles Sevcik equation [22]) valid for reversible systems:

$$I_p = -0.4463\ n\ F\ S\ C^\circ \sqrt{\frac{nFD}{RT}}\ \sqrt{v} \qquad (14)$$

The linearity of I_p versus $v^{1/2}$ for each system is verified in Figure 6, which confirms that the electrochemical reduction and oxidation are controlled by the diffusion of the electroactive species in the solution.

The slopes of the straight line are at T = 1073 K:

For Eu(III) reduction: $\frac{I_{pc}}{\sqrt{v}} = -(0.0277 \pm 0.0002)\ A\ s^{1/2}\ V^{-1/2}$ (15)

For Eu(II) oxidation: $\frac{I_{pa}}{\sqrt{v}} = (0.0273 \pm 0.0002)\ A\ s^{1/2}\ V^{-1/2}$ (16)

Using Eq. (14) and the concentration values [Eu(III)] and [Eu(II)] determined above (§ 4.1), the diffusion coefficients at T = 1073 K were found to be:

$D_{Eu(III)} = (3.18 \pm 0.02)\ 10^{-9}\ m^2\ s^{-1}$

$D_{Eu(II)} = (4.69 \pm 0.02)\ 10^{-9}\ m^2\ s^{-1}$

4.3.2. Using chronopotentiometry

Chronopotentiometry can also be used to determine the diffusion coefficients due to the limitation of the process by the diffusion of species in the solution, as demonstrated in § 3.3. From these data and by applying the Sand's equation (equation (7)), we obtained, at 1073 K, [Eu(II)] = 0.0448 mol kg^{-1} and [Eu(III)] = 0.0552 mol kg^{-1}:

$I_c \sqrt{\tau} = -(0.0168 \pm 0.0002)\ A\ s^{1/2}$ (17)

$I_a \sqrt{\tau} = (0.0165 \pm 0.0002)\ A\ s^{1/2}$ (18)

Using Eq. (7), the Eu(III) and Eu(II) diffusion coefficients at several temperatures have been calculated. At T = 1073 K, the average values were found to be very close to the one determined by cyclic voltammetry:

$D_{Eu(III)} = (3.21 \pm 0.02)\ 10^{-9}\ m^2\ s^{-1}$

$D_{Eu(II)} = (4.71 \pm 0.02)\ 10^{-9}\ m^2\ s^{-1}$

These values are in the same order of magnitude than diffusion coefficients of other lanthanide ions determined in the same medium in our laboratory [23-25].

4.3.3 Variation of the diffusion coefficients with temperature

Table 3 reports the value of the diffusion coefficients measured at four different temperatures (1073, 1093, 1113 and 1143 K). The data obey the following relationship (Arrhenius' law) for both species:

$$D = D^\circ \exp\left(-\frac{E_a}{RT}\right) \qquad (19)$$

where E_a is the activation energy in J mol^{-1} and D° is the pre-exponential factor.

The linearity of the evolution of ln D versus 1/T is observed in Figure 7. The temperature dependence of the diffusion coefficients are:

$$\ln D_{Eu(III)} = 22.54 - \frac{45020}{T}$$

$$\ln D_{Eu(II)} = 29.67 - \frac{52330}{T}$$

where D is in $cm^2\ s^{-1}$ and T in K.

From this relationship, the values of the activation energy are found to be 374.3 kJ mol^{-1} and 435.1 kJ mol^{-1} for Eu(III) and Eu(II) respectively.

5. Conclusions

The electrochemical behaviour of EuF_3 was studied in the LiF-CaF_2 medium using an inert molybdenum electrode. The electrochemical characterization highlighted that an addition of EuF_3 in the melt spontaneously led to the formation of an equilibrium between Eu(III) and Eu(II) species, at a concentration ratio depending on the operating temperature. The formal standard potential of the Eu(III)/Eu(II) system was determined, it indicates a large potential range of stability of Eu(II): this has to be taken into account in the frame of the chemistry of molten salts used as solvents for nuclear fuels, since most of the other Ln (e.g. Ce, Gd, Nd) are stable as a unique Ln(III) valence.

The kinetic investigation by electrochemical methods showed that the Eu(III)/Eu(II) electrochemical system is limited by the diffusion of electroactive species in solution. The diffusion coefficients of Eu(III) and Eu(II) were calculated by cyclic voltammetry and chronopotentiometry and showed a temperature dependence according to Arrhenius' law.

An important fact is that the electrochemical reduction of Eu(II) into Eu metal was not observed on the inert molybdenum cathode, due to the prior reduction of Li(I) ions from the solvent. This feature is very similar to the Sm system, which also exhibit a Sm(III)/Sm(II) transition within the electrochemical window, while the reduction of Sm(II) into Sm metal is hindered by the solvent reduction [23].

This article therefore demonstrates that Eu metal cannot be obtained in molten LiF-CaF_2 by electrochemical reduction of dissolved Eu ions on an inert electrode, preventing the extraction of Eu compounds from this melt. This fact is very likely to be also valid in other usual binary or ternary fluoride mixtures such as LiF-NaF, FLiNaK, LiF-ThF_4, etc., since they exhibit a smaller electrochemical window. However, other routes aiming at Eu electrochemical extraction can be envisaged. Two alternative ways, namely the use of a

reactive cathode and/or the electrochemical co-reduction with another cation, could allow precipitating this element into the form of an intermetallic compound. These processes will be evaluated in future work.

Acknowledgments

The authors express their thanks to the French CNRS PACEN program for the financial support of this work.

References

[1] J.P. Ackerman, Ind. Eng. Chem. Res. 30 (1991) 141.

[2] H.P. Nawada, K. Fukuda, J. Phys. Chem. Solids 66 (2005) 647.

[3] S. Delpech, E. Merle-Lucotte, D. Heuer, M. Allibert, V. Ghetta, C. Le Brun, X. Doligez, G. Picard, J. Fluorine Chem. 130 (2009) 11.

[4] P. Taxil, L. Massot, C. Nourry, M. Gibilaro, P. Chamelot, L. Cassayre, J. Fluorine Chem. 130 (2009) 94.

[5] P. Chamelot, L. Massot, C. Hamel, C. Nourry, P. Taxil, J. Nucl. Mat. 360 (2007) 64.

[6] S.A. Kuznetsov, L. Rycerz, M. Gaune-Escard, J. Nucl. Mat. 344 (2005) 152.

[7] S.A. Kuznetsov, M. Gaune-Escard, Electrochim. Acta 46 (2001) 1101.

[8] S.A. Kuznetsov, M. Gaune-Escard, J. Electroanal. Chem. 595 (2006) 11.

[9] D.M. Laptev, T.V. Kiseleva, N.M. Kulagin, V.F. Goryushkin, E.S. Voronkov, Russ. J. Inorg. Chem. 31 (1986) 1965.

[10] M.R. Bermejo, F. de la Rosa, E. Barrado, Y. Castrillejo, J. Electroanal. Chem. 603 (2007) 81.

[11] P. Chamelot, P. Taxil, B. Lafage, Electrochim. Acta 39 (17) (1994) 2571.

[12] L. Massot, P. Chamelot, F. Bouyer, P. Taxil, Electrochim. Acta 47 (12) (2002) 1949.

[13] T.B. Massalski, H. Okamoto, P.R. Subramanian, L. Kacprzak, Binary Alloy Phase Diagrams, 2nd ed., ASM International, Ohio (1990).

[14] Y. Berghoute, A. Salmi, F. Lantelme, J. Electroanal. Chem. 365 (1994) 171.

[15] R.J.M. Konings, A. Kovács, The Handbook on Physics and Chemistry of Rare Earths, Elsevier Science (2003) 147.

[16] S. Bratsch, H.B. Silber, Polyhedron 1 (1982) 219.

[17] L. Ramaley, M.S. Krause, Anal. Chem. 41 (1969) 1362.

[18] J.G. Osteryoung, J.J. O'Dea, Electroanal. Chem. 14 (1986) 209.

[19] P. Chamelot, P. Palau, L. Massot, A. Savall, P. Taxil, Electrochim. Acta 47 (2002) 3423.

[20] P. Chamelot, B. Lafage, P. Taxil, Electrochim. Acta 43 (5–6) (1997) 607.

[21] R.K. Jain, H.C. Gaur, B.J. Welch, J. Electroanal. Chem. 79 (1977) 211.

[22] A.J. Bard, R.L. Faulkner, Electrochemical methods: Fundamentals and Applications, Wiley, New York, 1980.

[23] L. Massot, P. Chamelot, P. Taxil, Electrochim. Acta 50 (2005) 5510-5517.

[24] C. Nourry, L. Massot, P. Chamelot, P. Taxil, Electrochim. Acta 53 (2008) 2650-2655.

[25] C. Hamel, P. Chamelot, P. Taxil, Electrochim. Acta 49 (2004) 4467-4476.

Legend of figures

Fig. 1:

Typical cyclic voltammogram of the $LiF\text{-}CaF_2\text{-}EuF_3$ system at 100 mV s^{-1} and T = 1073 K.

Working El.: Mo (S = 0.315 cm^2); *Auxiliary El.:* vitreous carbon; *Reference El.:* Pt

Fig. 2:

Square Wave Voltammograms of the $LiF\text{-}CaF_2\text{-}EuF_3$ melt. Frequency: 25 Hz, T = 1073 K.

Working El.: Mo (S = 0.315 cm^2); *Auxiliary El.:* vitreous carbon; *Reference El.:* Pt

Fig. 3:

Typical chronopotentiograms of the system $LiF\text{-}CaF_2$ for Eu(III) reduction (I_{app} = -15 mA) and Eu(II) oxidation (I_{app} = 10 mA) at 1073 K.

Working El.: Mo (S = 0.315 cm^2); *Auxiliary El.:* vitreous carbon; *Reference El.:* Pt

Fig. 4:

Variation of $I.\tau^{1/2}\ C^{-1}$ versus the intensity at 1073 K.

Working El.: Mo (S = 0.315 cm^2); *Auxiliary El.:* vitreous carbon; *Reference El.:* Pt

Fig. 5:

Linear relationship between the Eu(III) reduction and Eu(II) oxidation peaks current densities and the corresponding Eu(III) and Eu(II) concentrations in the melt obtained by square wave voltammetry at 25 Hz.

Working El.: Mo (S = 0.315 cm^2); *Auxiliary El.:* vitreous carbon; *Reference El.:* Pt

Fig. 6:

Linear relationship of Eu(III) reduction and Eu(II) oxidation peaks current densities versus the square root of the scanning potential rate at T = 1073 K.

Working El.: Mo (S = 0.315 cm^2); *Auxiliary El.:* vitreous carbon; *Reference El.:* Pt

Fig. 7:

Linear relationship of the logarithm of Eu(III) and Eu(II) diffusion coefficients versus the reverse of the absolute temperature.

Table 1:

Variation of the [Eu(III)]/[Eu(II)] equilibrium constant with the temperature.

Table 2:

Variation of the Eu(III)/Eu(II) formal standard potential with the temperature.

Table 3:

Variation of the Eu(III) and Eu(II) diffusion coefficients with the temperature using cyclic voltammetry and square wave voltammetry measurements.

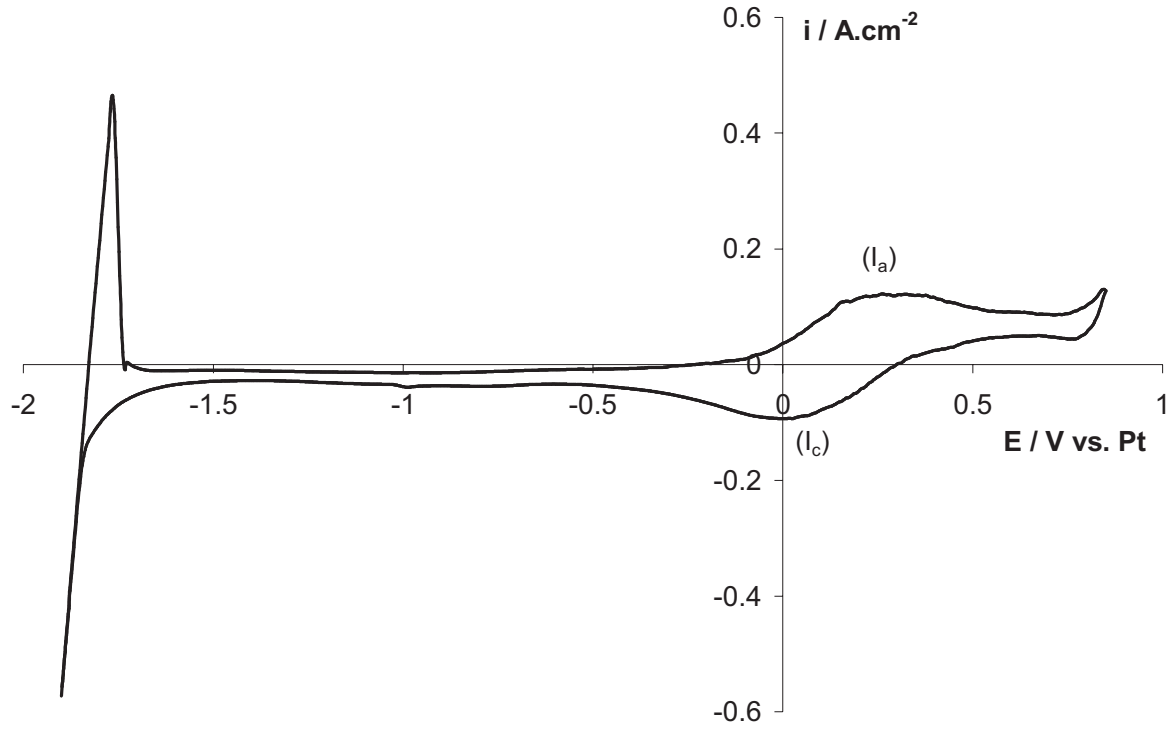

Figure 1

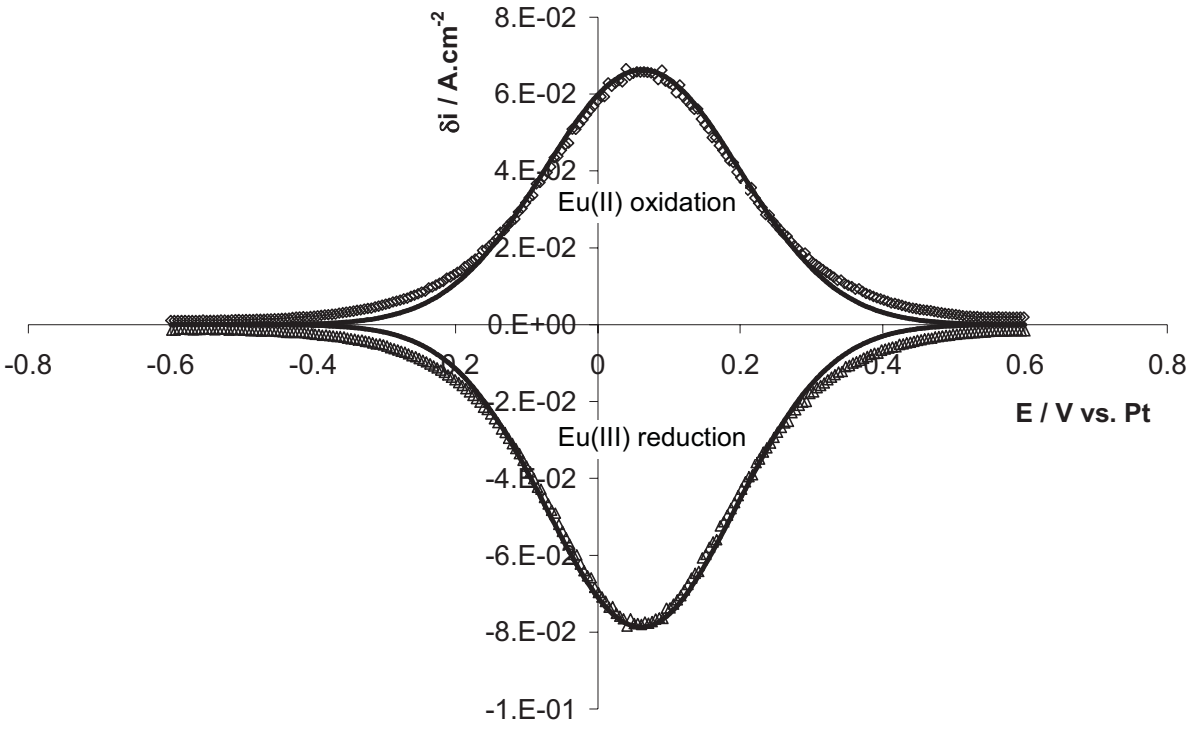

Figure 2

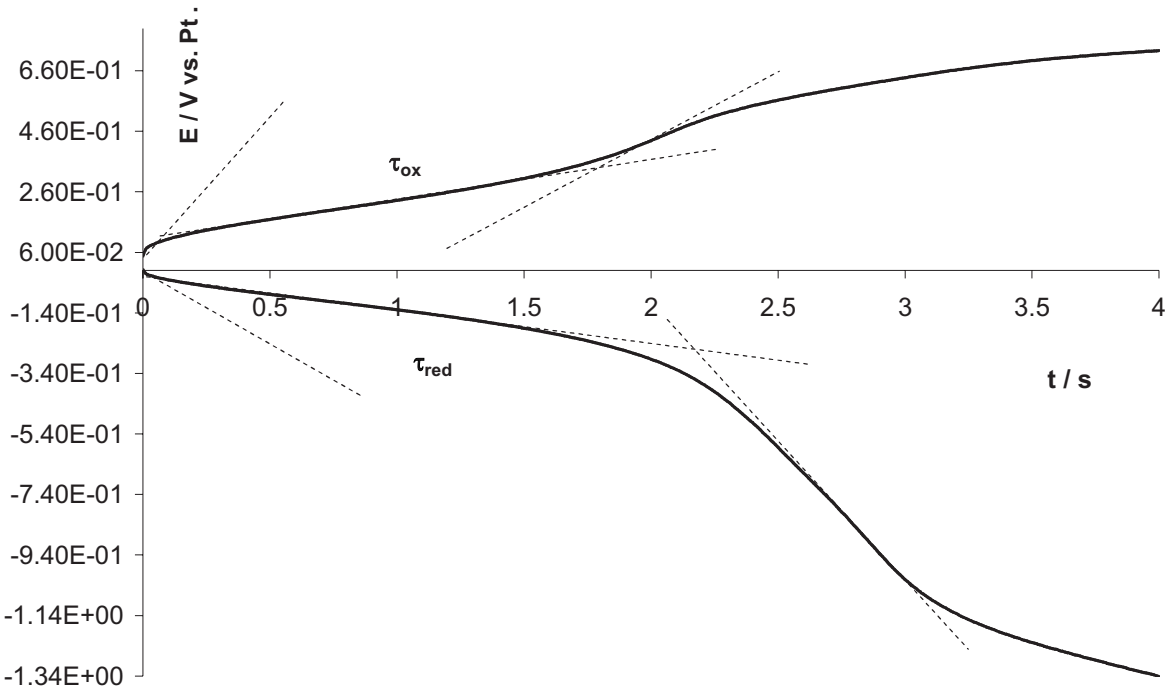

Figure 3

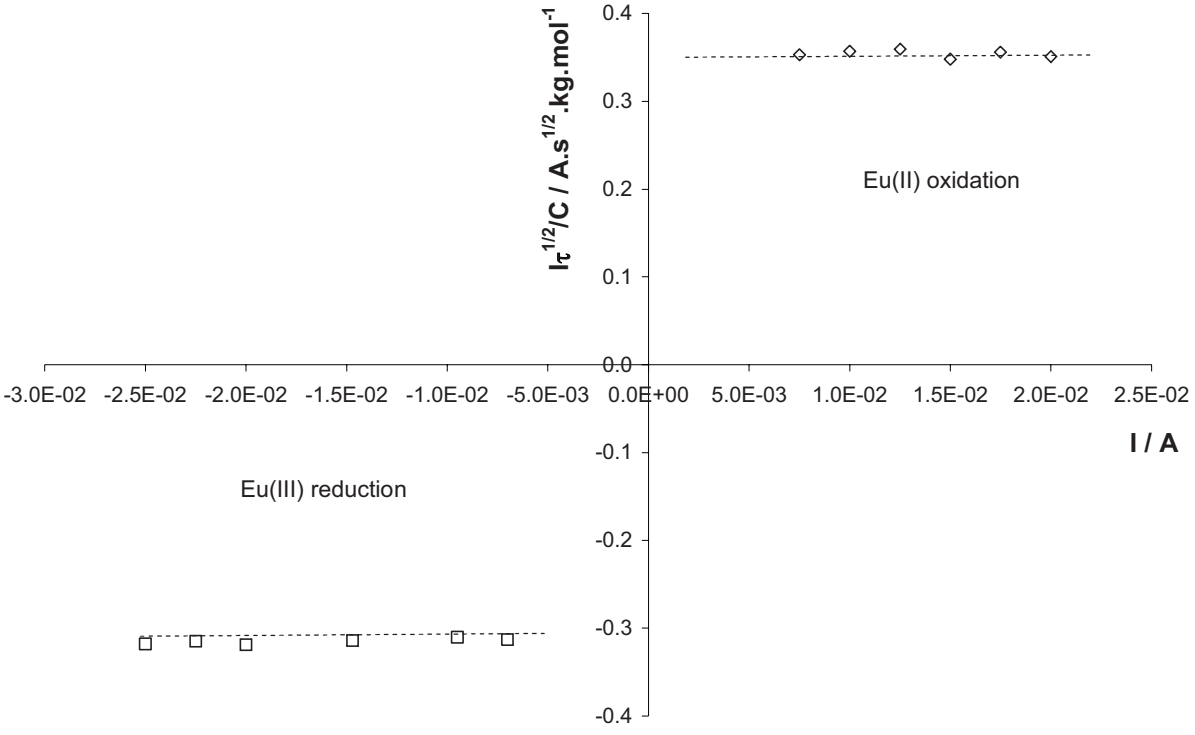

Figure 4

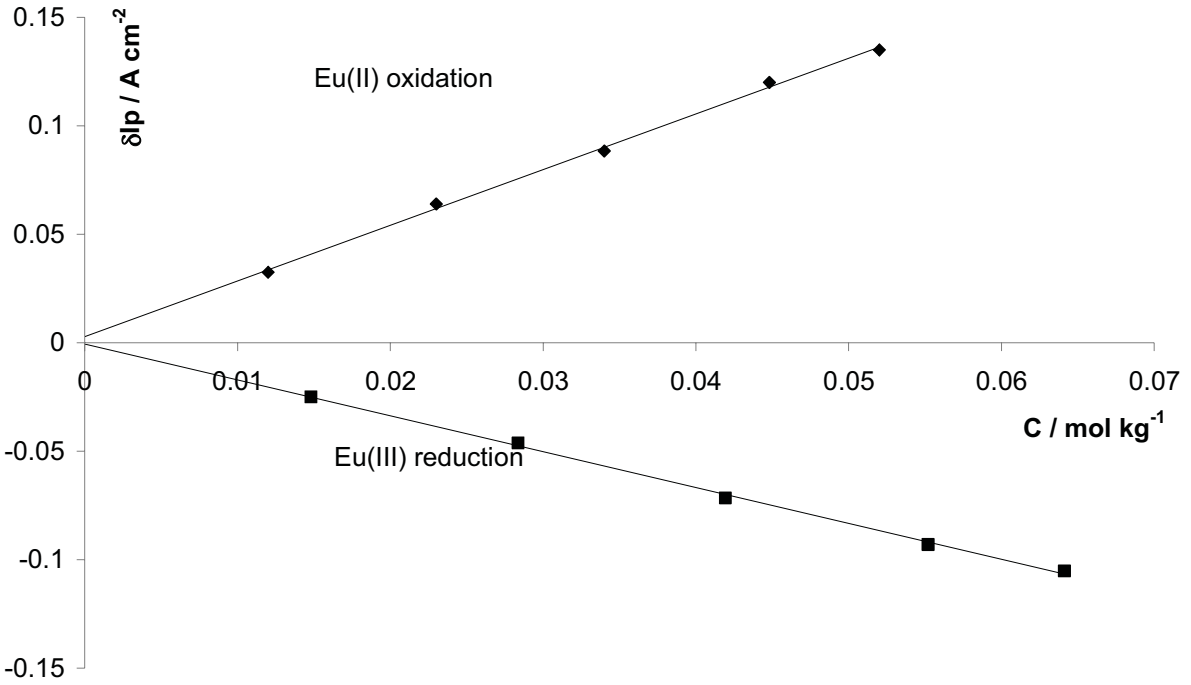

Figure 5

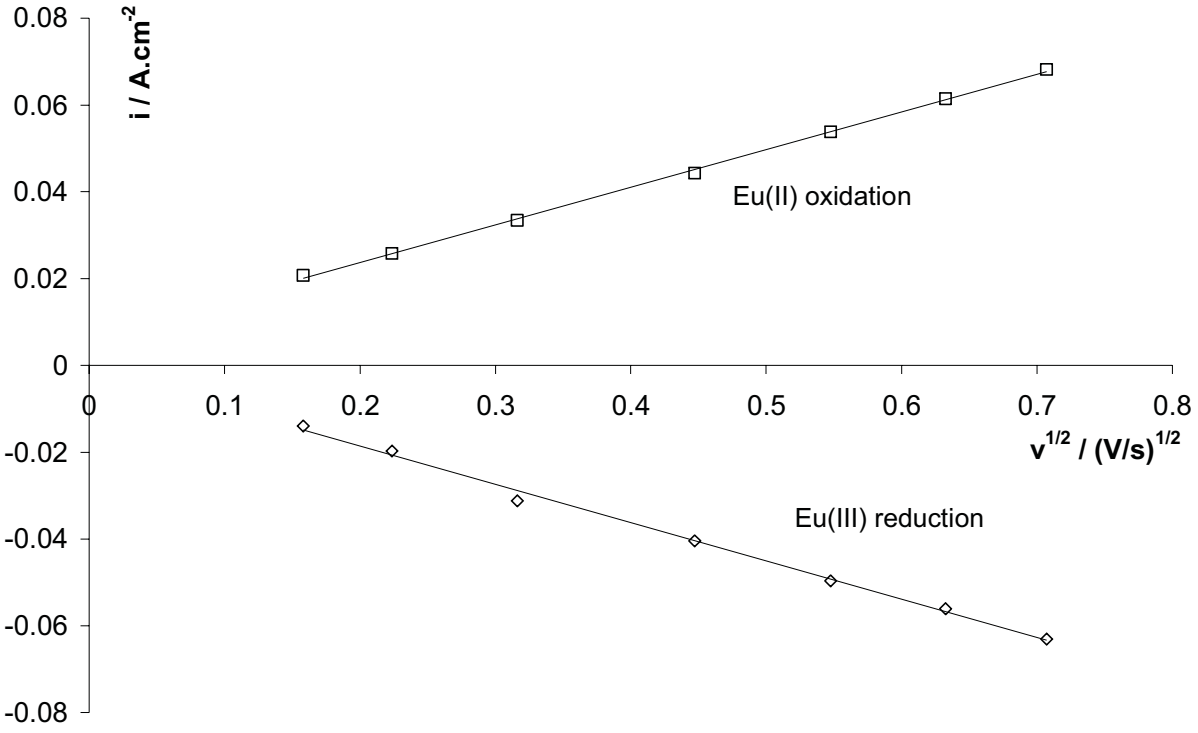

Figure 6

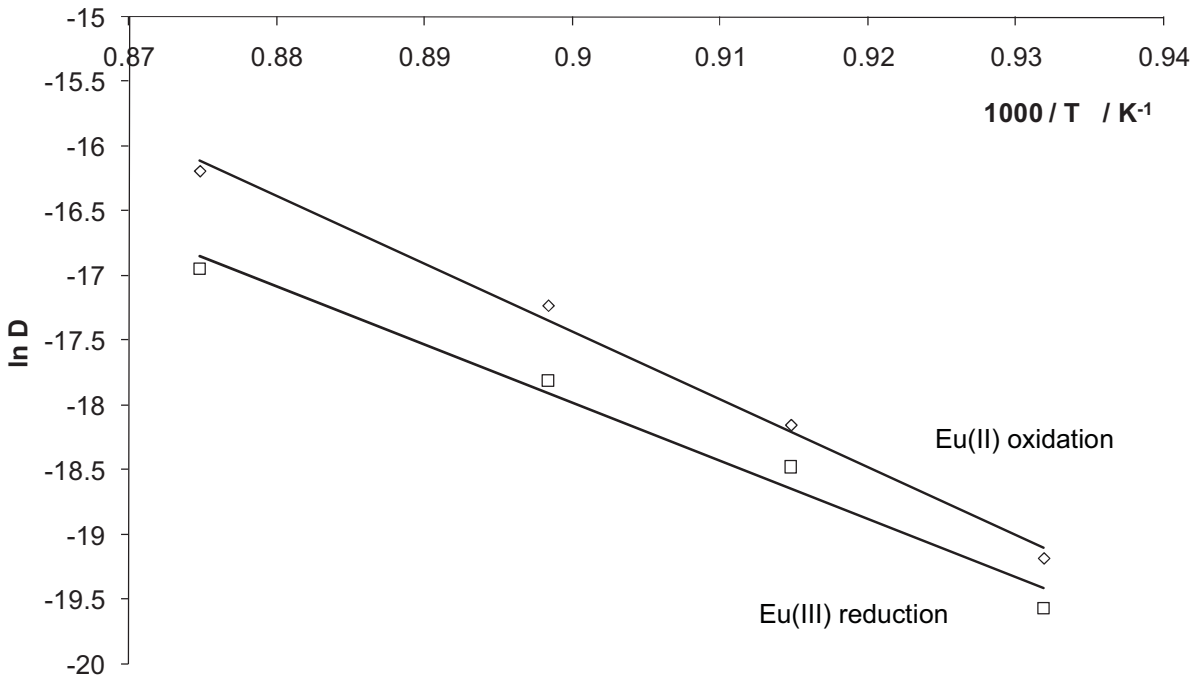
-15
-15.5
-16
-16.5
-17
-17.5
-18
-18.5
-19
-19.5
-20
ln D
0.87
0.88
0.89
0.9
0.91
0.92
0.93
0.94
1000 / T / K-1
Eu(II) oxidation
Eu(III) reduction

Figure 7

Temperature / K	$\frac{[Eu(II)]}{[Eu(III)]}$ ratio
1073	0.811 ± 0.02
1093	0.866 ± 0.02
1113	0.900 ± 0.02
1143	0.970 ± 0.02

Table 1

Temperature / K	$E^{*}_{Eu(III)/Eu(II)}$ **/ V vs. F_2/F^-**
1073	-3.53 ± 0.01
1093	-3.46 ± 0.01
1113	-3.40 ± 0.01
1143	-3.33 ± 0.01

Table 2

Temperature / K	Cyclic voltammetry		Chronopotentiometry	
	$D_{Eu(II)}$ **$* 10^9$ ($m^2 s^{-1}$)**	$D_{Eu(III)}$ **$*10^9$ ($m^2 s^{-1}$)**	$D_{Eu(II)}$ **$* 10^9$ ($m^2 s^{-1}$)**	$D_{Eu(III)}$ **$*10^9$ ($m^2 s^{-1}$)**
1073	4.69	3.18	4.71	3.21
1093	13.10	9.47	13.13	9.49
1113	33.01	18.47	33.02	18.50
1143	93.10	43.71	93.11	43.75

Table 3